ANL-80-46

MASTER

ANL-80-46

MATERIALS TECHNOLOGY FOR COAL-CONVERSION PROCESSES

Progress Report for January—March 1980

ARGONNE NATIONAL LABORATORY

ARGONNE NATIONAL LABORATORY, ARGONNE, ILLINOIS

Prepared for the Office of Fossil Energy
U. S. DEPARTMENT OF ENERGY
under Contract W-31-109-Eng-38

Distribution Categories:
Coal Conversion and Utilization:
Coal Gasification (UC-90c)
Direct Combustion of Coal (UC-90e)
Materials and Components (UC-90h)

ANL-80-46

ARGONNE NATIONAL LABORATORY
9700 South Cass Avenue
Argonne, Illinois 60439

MATERIALS TECHNOLOGY FOR COAL-CONVERSION PROCESSES

Progress Report for
January—March 1980

William A. Ellingson
Program Manager

Materials Science Division

June 1980

Most recent reports in this series

ANL-79-23	October—December 1978
ANL-79-56	January—March 1979
ANL-79-93	April—June 1979
ANL-80-12	July—December 1979

TABLE OF CONTENTS

TABLE OF CONTENTS (continued)

LIST OF FIGURES

LIST OF FIGURES (continued)

LIST OF TABLES

MATERIALS TECHNOLOGY FOR COAL-CONVERSION PROCESSES
Progress Report for
January—March 1980

HIGHLIGHTS

Task A -- Evaluation of Ceramic Refractories for Slagging Gasifiers *(C.R. Kennedy, S.W. Kreis, and R.J. Fousek)*

The mechanisms responsible for the corrosion of the refractories from test run 11 have been identified using SEM and metallography. The high-alumina refractory reacted with the basic slag to produce calcium hexaluminate. As the chromia content of the alumina-chromia refractories increased from 10 to 32%, the primary reaction product changed from calcium hexaluminate to spinel, and the corrosion resistance was markedly increased. Free magnesia in the magnesia-chrome and magnesia-spinel refractories was preferentially dissolved.

Test run 12 has nearly been completed. This test will evaluate the compatibility of a high-iron oxide acid slag with chrome-containing refractories.

Task C -- Development and Application of Nondestructive Evaluation Methods for Coal-conversion Processes *(W.A. Ellingson and T.A. Youngdahl)*

The major activity during this period has been further field evaluation of the high-temperature ultrasonic erosion scanner. The high-temperature scanner was operated at the Solvent Refined Coal (SRC) coal liquefaction plant in Tacoma, WA, and data suggested repeatability of system measurements to be ± 0.025 mm. Both the SRC and the Morgantown erosion-scanning systems are now directly connected to automatic, computer-controlled data-acquisition systems. Wear data obtained with the scanner at SRC suggest that the wear rate was higher in new 1-1/2-in. piping than in 2-in. piping used simultaneously in the same line. The 2-in. piping had been exposed previously to the process stream. The lower rate of wear in the larger pipe is probably a result of a lower stream velocity and the presence of a hard reaction layer that SRC plant personnel have noted on stainless steel exposed to the high-temperature process fluid. Analysis of a chart record showed that the ANL scanner at Morgantown successfully monitored wear of the cyclone (maintained at nominally 540°C) during the run of November-December 1979.

Final arrangements were made with Exxon to install high-temperature erosion-monitoring equipment at the Baytown, TX coal liquefaction plant. Also, agreement has been reached with Exxon on most of the details regarding field testing of the passive acoustic system for blockage-valve leak detection.

Task D -- Corrosion Behavior of Materials in Coal-conversion Processes *(K. Natesan)*

The experimental program to evaluate the effect(s) of multicomponent gas environments on the corrosion and uniaxial tensile properties of four high-chromium alloys has been completed. The results are being analyzed and will be summarized in a topical report. A review of the corrosion behavior of commercially available alloys showed that a number of them exhibit acceptible corrosion rates of ~ 0.6 mm y^{-1}, based on 10,000-h exposures to complex gas mixtures. However, the experiments in these studies were conducted at excess oxygen-parameter values of $\sim 10^3$ or higher; the alloys exposed under these conditions are expected to develop protective oxide scales, and the long exposures used will only establish the susceptibility of a given alloy to breakaway corrosion. Data are also needed on the corrosion behavior of materials in environments with excess oxygen-parameter values below 10^3, since most coal-gasification processes will expose materials to a wide range of oxygen partial pressures.

Experiments have been initiated to develop information on material behavior in low-Btu gasification and combustion environments for heat-exchanger and gas-turbine applications.

Task E -- Erosion Behavior of Materials in Coal-conversion Processes *(J.Y. Park and W.J. Shack)*

A room-temperature erosion calibration test was performed on 1015 carbon steel, Type 304 stainless steel, Incoloy 800, RA310 stainless steel, and Stellite 6B using 100-grit size (150-μm) alumina at an impingement velocity of 22 m/s and angles of 6 tc 36°. The erosion rate (mass loss/mass impacted) was found to be 0.03-0.09 mg/g. These results are comparable to those obtained by other investigators.

Task F -- Failure Analysis *(D.R. Diercks, S. Greenberg, J.Y.N. Wang, G.M. Dragel, and J.E. Slattery)*

Seven experimental thermowells prepared for trial exposure in the IGT U-Gas Pilot Plant have been completed and are presently in place awaiting start-up of that plant. An examination of tubing and compressor diaphragm samples from the GFETC coal-liquefaction continuous-process unit has been completed; cracks were detected in two of the three diaphragm samples analyzed. An extensive investigation of a failed internal solids transfer line from the IGT HYGAS Pilot Plant is presently under way. Initial results indicate that the failure was due to severe localized sulfidation attack on the high-nickel Inconel 182 weld metal used to fabricate the line. A failed thermocouple assembly from the HYGAS plant is also being examined, but the cause of failure for this component has not yet been identified.

MATERIALS TECHNOLOGY FOR COAL-CONVERSION PROCESSES
Progress Report for
January—March 1980

FOREWORD

This broad-base materials engineering program, begun in 1974, includes studies on ceramic (refractory) and metallic materials presently being used or intended for use in coal-conversion processes. The program entails nondestructive testing, failure analysis, and studies of erosive wear, corrosion, and refractory degradation. Appropriate laboratory and field experiments are integrated such that the results have impact on present pilot- and demonstration-plant and proposed full-scale designs. This report, for the period January-March 1980, presents the technical accomplishments of the program.

ABSTRACT

Analysis of recent refractory-slag interaction tests suggests that as the chromia content is increased from 10 to 32%, the primary reaction product changes from calcium hexaluminate to spinel, significantly increasing the corrosion resistance of the refractory.

Field reliability of the high-temperature ultrasonic erosion scanner was demonstrated at both a coal liquefaction plant (SRC at Tacoma, WA) and a coal gasification plant (Morgantown, WV). Continuous high-temperature operation has been demonstrated and an accuracy of ± 0.025 mm seems achievable.

Equipment has been ordered for field tests of passive acoustic systems at Exxon. This includes a four-channel tape recorder, differential amplifiers, and signal conditioners.

Corrosion studies have been completed on effects of multicomponent gas environments on corrosion mechanisms and uniaxial tensile properties of Fe-Ni-Cr alloys. Results of these and other tests utilizing 10,000-h exposures suggest that corrosion rates of 0.6 mm/y can be expected.

Failure analysis activities included studies of compressor diaphragms from the Grand Forks Energy Technology Center coal-liquefaction continuous-process unit. Cracks were found in two of the three diaphragms. Failure of an internal solids transfer line from HYGAS appears to have been caused by severe localized sulfidation of the high-nickel Inconel 182 weld metal used to fabricate the line.

In addition to these research activities, program plans were prepared and submitted for FY 1981 and FY 1982.

INTRODUCTION

Economical conversion of coal into clean and usable alternate fuels will be advanced through the use of durable materials systems. The technical information base applicable to materials selection in plant design for the operating environments of various coal-conversion processes is extremely limited. Hence, reliable selection and lifetime-prediction methods for materials under these conditions are not available. This program is designed to provide part of the materials information necessary for successful operation of coal-conversion systems. The present report is the twentieth progress report submitted by ANL to the Office of Advanced Research and Technology, Office of Fossil Energy under Project Number 7106, "Materials Technology for Coal-conversion Processes".

The project includes five tasks: (A) Evaluation of commercial refractories exposed to coal slag under conditions typical of those encountered in slagging gasification processes; (C) development, evaluation, and application of nondestructive evaluation methods for coal-conversion systems; (D) evaluation of the corrosion behavior of commercial alloys; (E) development of analytical models to predict the erosive-wear behavior of materials used in coal-conversion plants; and (F) analysis of failed coal-conversion plant components.

Task A -- Evaluation of Ceramic Refractories for Slagging Gasifiers
(C.R. Kennedy, S.W. Kreis, and R.J. Fousek)

Metallographic and SEM examinations of selected refractories (see Table I) from test run 11 have been completed and are presented below. In this test[1], the refractories were exposed to a basic coal slag (base-to-acid ratio equal to 1.5) at 1500°C for ~ 500 h.

1. Fused-cast Alumina (Number 2)

The fused-cast alumina refractory was attacked by the slag, which consisted of gehlenite ($Ca_2Al_2SiO_7$) and glass, to produce a primary reaction product of calcium hexaluminate needles (see Fig. 1) with minor amounts of Fe-rich spinel. Despite the fact that calcium hexaluminate has a larger unit volume than alumina and despite some tendency towards intergranular corrosion, no observable swelling of the refractory accompanied the corrosion reaction.

2. Sintered Alumina-Chromia (Number 16)

The 90% Al_2O_3-10% Cr_2O_3 refractory also reacted with the slag to produce calcium hexaluminate and minor amounts of spinel (Fig. 2). However, owing to extensive intergranular formation of calcium hexaluminate, the outer 20 mm of the brick exhibited substantial swelling. SEM examination (Fig. 3) revealed that the calcium hexaluminate needles contained some Cr in solid solution, i.e., $Ca(Al_{12-x}Cr_x)O_{19}$, and that the spinel consisted primarily of $Fe(Fe,Al,Cr)_2O_4$-type.

3. Sintered Alumina-Chromia (Number 852)

The alumina-16.6% chromia was substantially more resistant to the basic coal slag than was the alumina-10% chromia refractory (number 16). Figure 4 shows that, in addition to calcium hexaluminate, significant amounts of spinel were produced when the slag and the refractory reacted. Also evident in Fig. 4 is the lack of intergranular attack and the small depth of alteration as compared with number 16 (Fig. 2). In agreement with the previous observations, no swelling was observed in this brick.

4. Fused-cast Alumina-Chromia (Number 280)

The fused-cast alumina-32% chromia demonstrated markedly better corrosion resistance than either the fused-cast alumina or the sintered alumina-10% chromia refractory. Examination of the slag-refractory interface revealed that a dense $(Mg,Fe)(Al,Cr,Fe)_2O_4$-type spinel layer had formed, with no calcium hexaluminate detectable (Fig. 5). Since no $CaCr_{12}O_{19}$ compound has been found to exist in the CaO-Al_2O_3-Cr_2O_3-SiO_2 system, (see Ref. 2), it is apparent that at some chromia content between 16 and 32% in the refractory, sufficient chromia dissolves along with the alumina to inhibit the formation of the $Ca(Al_{12-x}Cr_x)O_{19}$ phase, with spinel forming instead.

5. Fused-cast Magnesia-Spinel (Number 317)

The as-received microstructure of this material consisted of periclase (MgO) grains surrounded by a spinel ($MgAl_2O_4$) matrix (Fig. 6). Posttest examination revealed that both phases underwent iron oxide enrichment, and that the periclase grains appeared to be more readily dissolved by the slag than the spinel matrix (Fig. 7). It should be noted, however, that the overall rate of attack was the second highest observed, exceeded only by the corrosion rate of the chemically bonded Al_2O_3-7.5% Cr_2O_3 refractory.

6. Sintered Magnesia-Chrome (Number 35)

As in the case of the magnesia-spinel refractory, the free magnesia appeared to be preferentially attacked by the slag (Fig. 8). Although substantial penetration by the slag was observed, the chrome-spinel phase was highly resistant to dissolution, unlike the magnesia-spinel phase in refractory number 317, and thus the overall rate of corrosion was low. Iron oxide enrichment of both phases near the slag-refractory interface was again observed.

Test run 12, which will evaluate the compatibility of a variety of chrome-containing refractories with a high-iron oxide (25%) acidic coal slag at 1575°C, was initiated on January 11, 1980. Shortly after the furnace reached operating temperature, a failure of a natural-gas flowmeter sight glass caused an automatic shutdown. Because of the potentially serious nature of this failure, a safety review of the apparatus and control systems was conducted. As a result of this review, new types of flowmeters were installed in the natural-gas lines and additional air-flow sensors were incorporated into the automatic shutdown system. An inspection of the refractories revealed that serious corrosion had already occurred in two types of carbon-impregnated brick after only ∿ 36 h at 1575°C. These refractories were removed from the unit and replaced with conventional alumina-chromia refractories. The furnace was restarted on February 22 but a leak in a water flowmeter caused a loss of cooling water to a burner and resulted in another shutdown on February 23. Examination of the burner revealed that it also had developed a leak, which had to be repaired. The furnace was started for the third time on March 25.

TABLE I. Composition of Refractories from Test Run 11
Selected for Posttest Examination

Refractory No.	Composition, wt %	Type
2	Al_2O_3(99)-Na_2O(0.5)	Fused-cast
16	Al_2O_3(89.7)-Cr_2O_3(10.0)	Sintered
852	Al_2O_3(81.1)-Cr_2O_3(16.6)-P_2O_5 (0.8)-SiO_2(0.5)-Fe_2O_3(0.5)-Na_2O(0.5)	Sintered
280	Al_2O_3(65)-Cr_2O_3(32)-FeO(1)-CaO(0.6)-MgO(0.6)	Fused-cast
35	MgO(60)-Cr_2O_3(15.5)-Al_2O_3(15) Fe_2O_3(7)-SiO_2(1.5)-CaO(1)	Sintered
317	MgO(65)-Al_2O_3(35)	Fused-cast

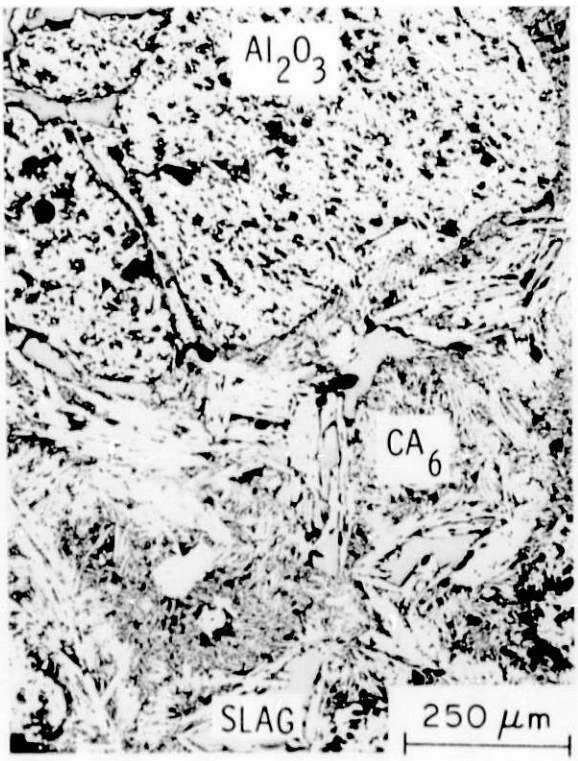

Fig. 1. Slag-Refractory Interface of a Fused-cast 99% Al_2O_3 Refractory (Number 2) Exposed to a Basic Coal Slag in Test Run 11. Slag (dark gray) has penetrated and reacted to form calcium hexaluminate (needle-shaped crystals). Shown at the top of the photograph is the unreacted refractory. ANL Neg. No. 306-79-557.

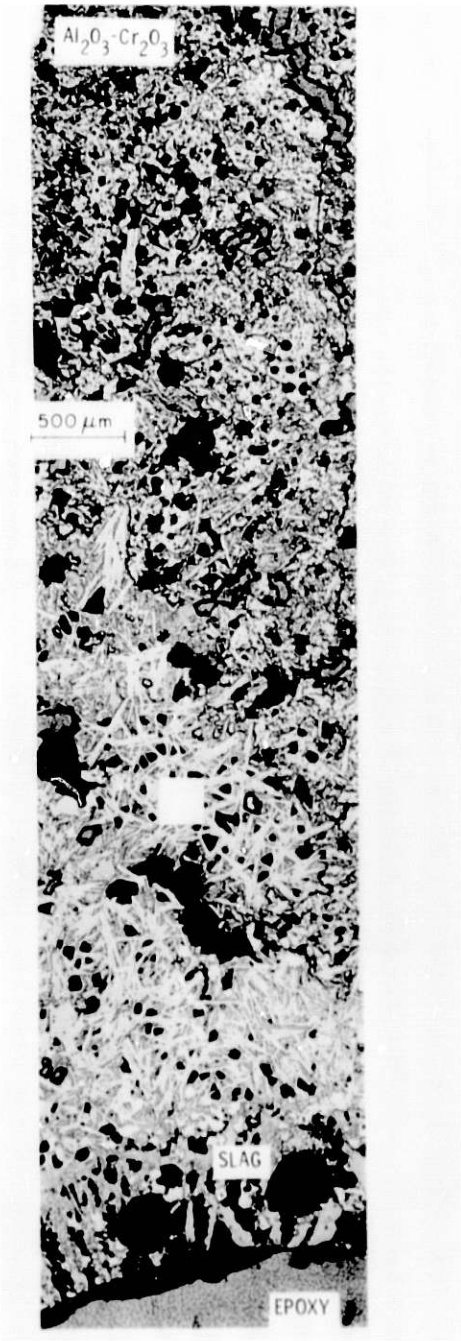

Fig. 2. Slag-Refractory Interface of a Sintered Alumina-Chromia Refractory (Number 16) Exposed to a Basic Coal Slag in Test Run 11. Note the intergranular attack, with the formation of calcium hexaluminate and minor amounts of spinel. ANL Neg. No. 306-80-210.

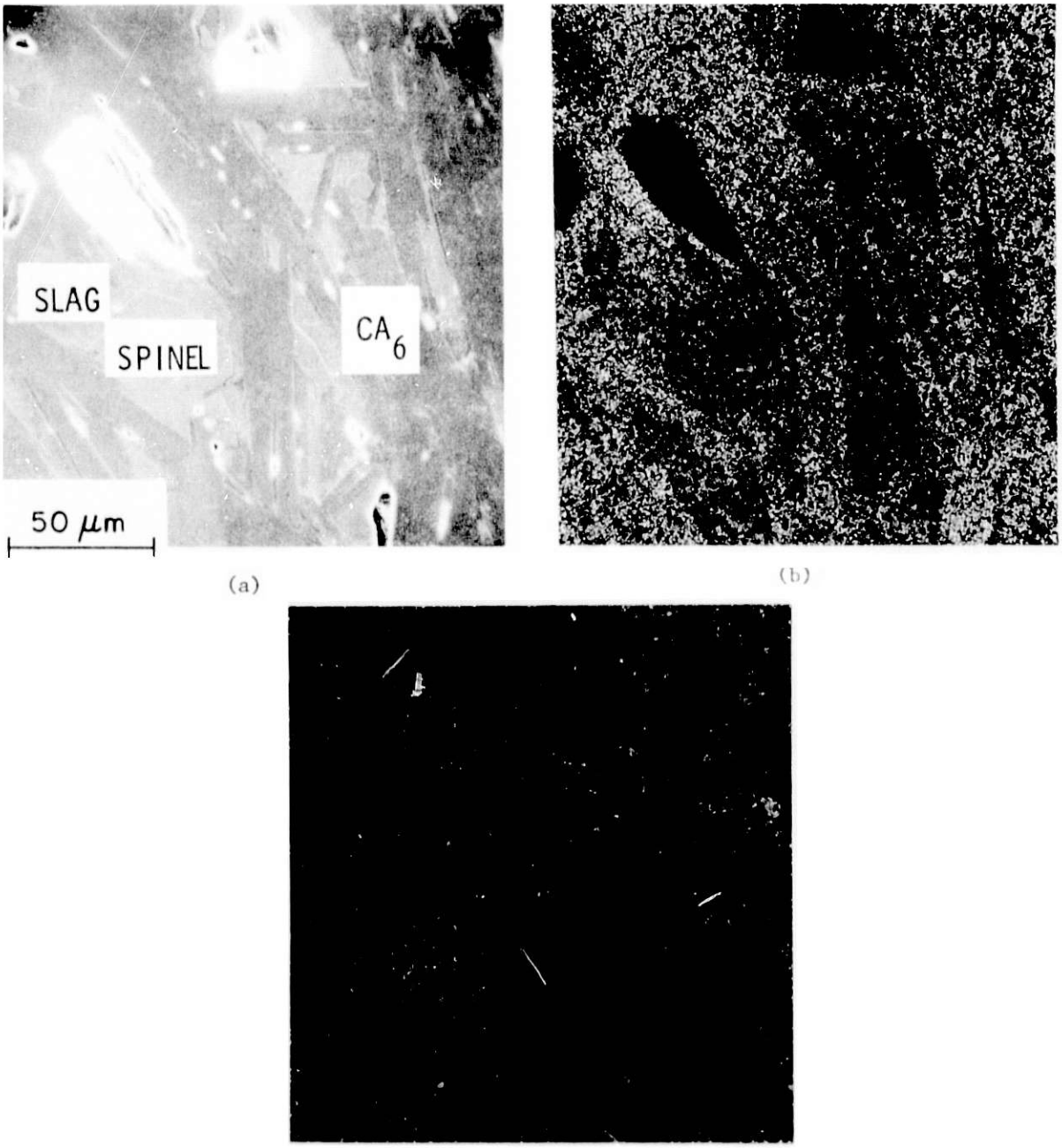

Fig. 3. SEM Photograph and Elemental Scans of the Slag-Refractory Reaction Products (Area Similar to the Lower Left of Fig. 2). (a) SEM, (b) Al, (c) Cr, (d) Fe, (e) Mg, (f) Ca, and (g) Si. Note that some Cr is in solution in the CA_6 phase. ANL Neg. Nos. 306-80-202, 200.

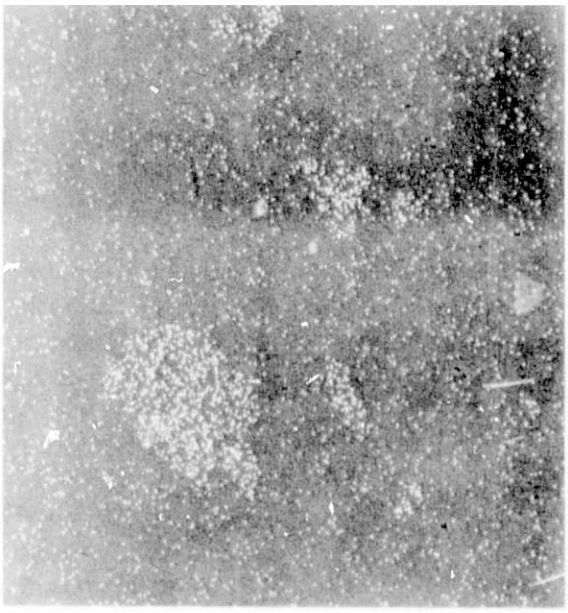

(d)

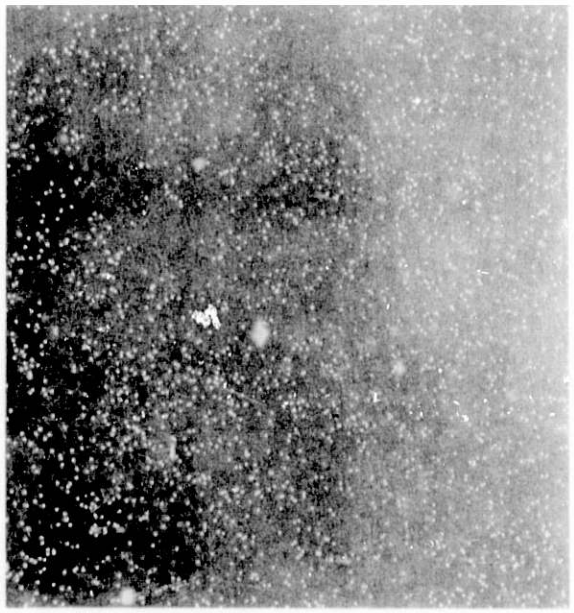

(e)

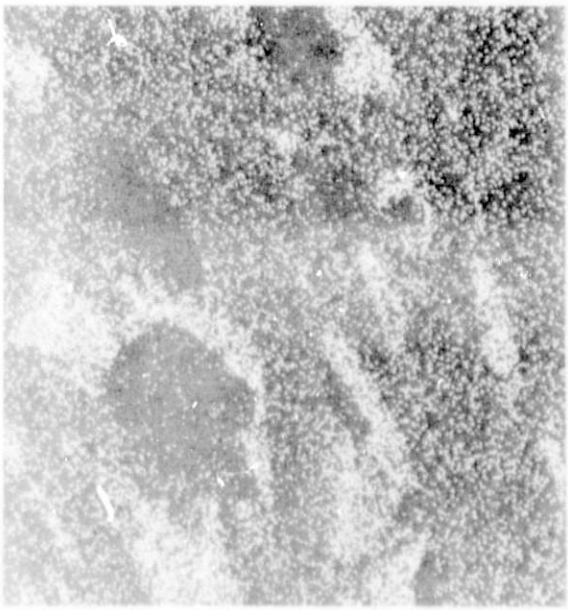

(f)

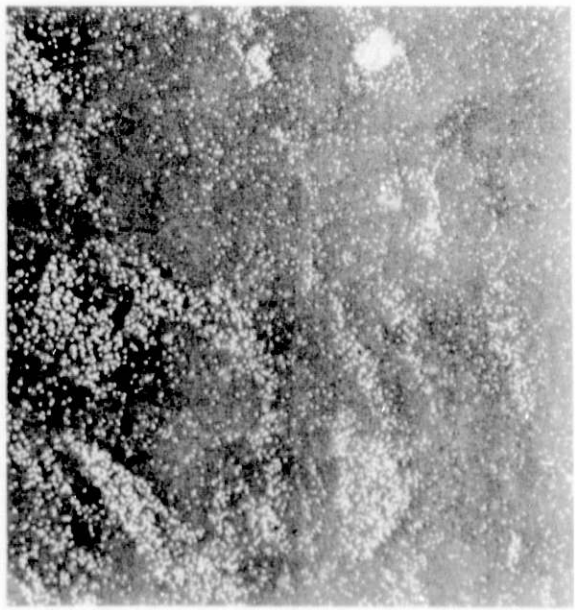

(g)

Fig. 3 (contd.)

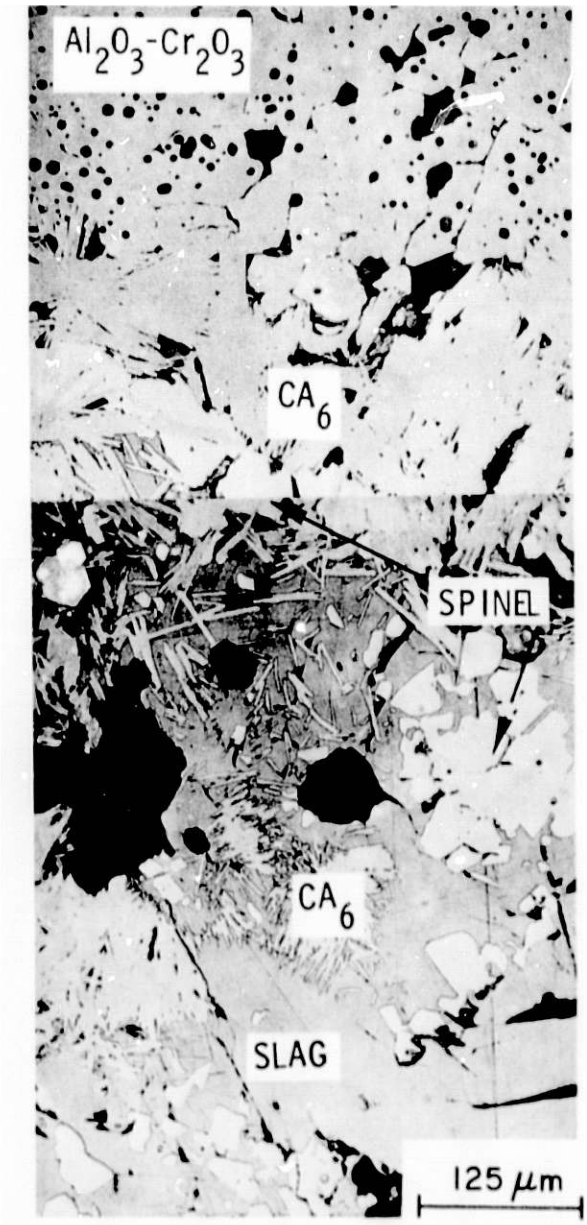

Fig. 4. Slag-Refractory Interface of a Sintered Alumina - 16.6% Chromia Refractory Exposed to a Basic Slag in Test Run 11. ANL Neg. No. 306-80-211.

Fig. 5. Slag-Refractory Interface of a Fused-cast Alumina - 32% Chromia Refractory Exposed to a Basic Coal Slag in Test Run 11. The slag, which did not adhere to the refractory, has reacted with it to produce a dense $(Mg,Fe)(Al,Cr,Fe)_2O_3$ spinel layer. ANL Neg. No. 306-79-559.

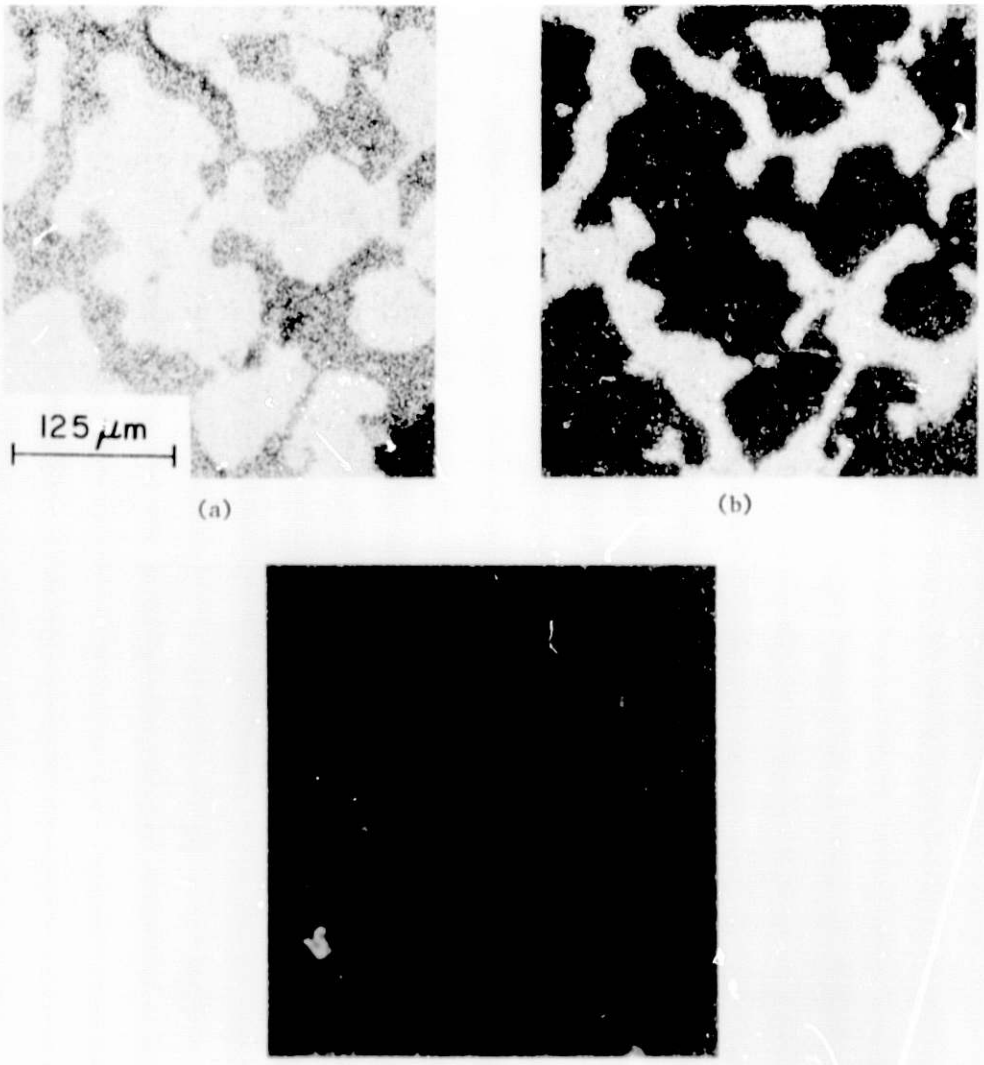

Fig. 6. As-received Microstructure of the Fused-cast Magnesia-Spinel Refractory (Number 317). (a) Mg scan, (b) Al scan, and (c) Fe scan. ANL Neg. No. 306-80-199.

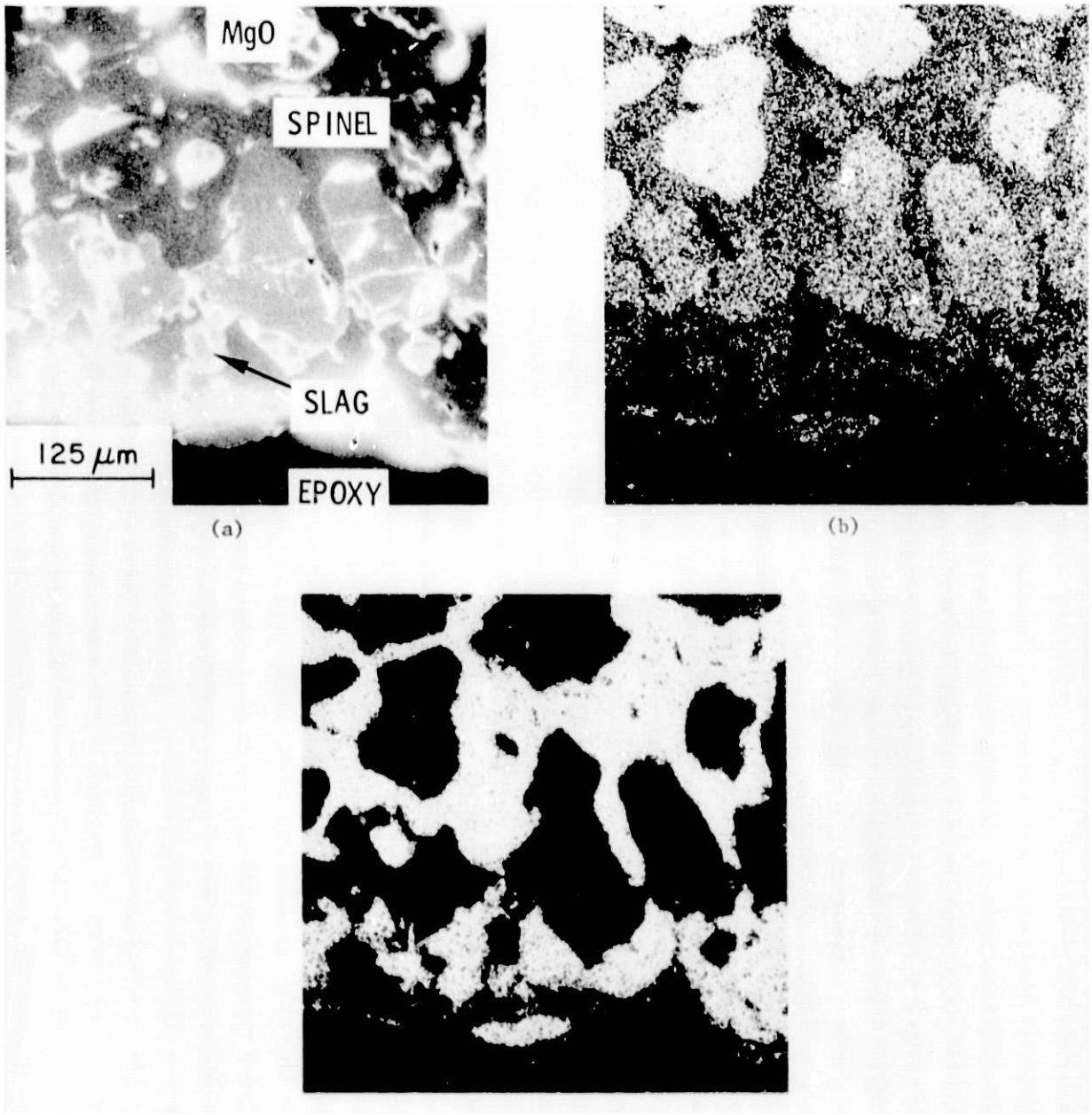

Fig. 7. Slag-Refractory Interface of the Fused-cast Magnesia-Spinel Refractory Exposed to a Basic Coal Slag in Test Run 11. (a) SEM photograph, (b) Mg scan, (c) Al Scan, (d) Fe scan, (e) Ca scan, and (f) Si scan. ANL Neg. Nos. 306-80-203, 201.

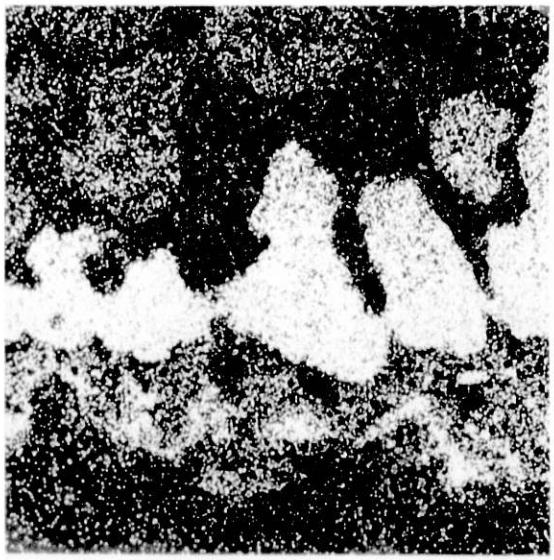

(d)

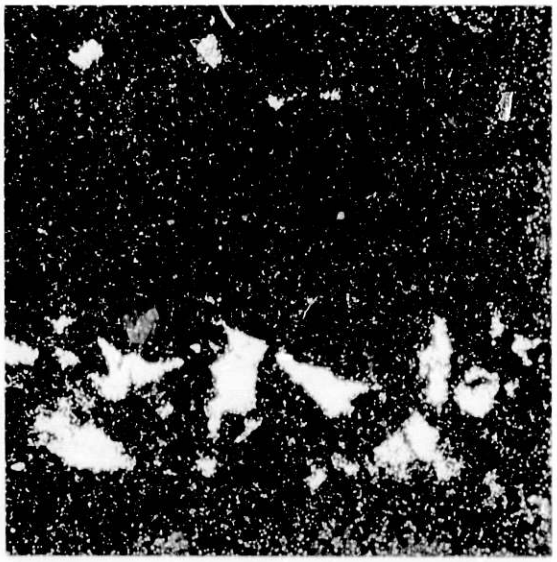

(e)

(f)

Fig. 7 (contd.)

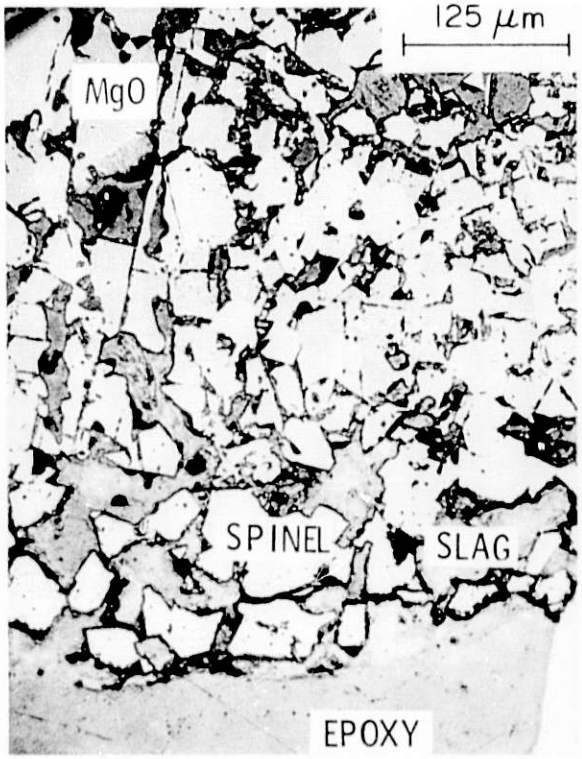

Fig. 8. Slag-Refractory Interface of a Sintered Magnesia-Chrome Refractory (Number 35) Exposed to a Basic Coal Slag in Test Run 11. ANL Neg. No. 306-80-209.

Task C -- Development and Application of Nondestructive Evaluation Methods for Coal-conversion Processes *(W.A. Ellingson and C.A. Youngdahl)*

1. Erosive Wear: Detection and Monitoring

a. Metallic Transfer Lines

(1) Ultrasonic Studies - Pilot Plants

(a) Solvent Refined Coal Liquefaction Plant

Ultrasonic monitoring of erosive wear of an erosion-corrosion (EC) loop and a slurry preheater at the Solvent Refined Coal (SRC) pilot plant was continued cooperatively by ANL and the Pittsburgh and Midway Coal Mining Company, which operates the plant. The wear results are based on measurements made in September 1979, before plant operations resumed, as compared with data obtained (1) during operation in December 1979, (2) during a shutdown in January 1980, and (3) after a subsequent de-coking treatment of the preheater. On each occasion, data were obtained from the remote scanning system.[3] In September 1979 and January 1980, direct-wall-contact data were also obtained for comparison with the scanner results.

The ultrasonically indicated wear at the EC loop between the time of start-up in November 1979 and the survey in December 1979 was described in the previous report.[3] Wear of up to 0.18 mm (7 mils) was evident at bends in the 1-1/2-in. piping, and little or no wear was seen in straight pipe runs. In 2-in. piping, which was present in a similar configuration in this loop, the wear was not significant (the apparent wear of 0.13 mm at waveguide no. 24 was not reproduced in later measurements). The results of the survey performed in January 1980 (see below) tend to confirm those of December 1979.

Table II shows the EC loop wear as of mid-January, as determined from ambient-temperature measurements made through the scanner: 0.20-0.25 mm (8-10 mils) of wear was indicated in the first bend of 1-1/2-in. piping, somewhat less wear in the last 1-1/2-in. pipe bend, and only 0-0.05 mm (2 mils) of thickness loss in straight runs. Only 0-0.08 mm (0-3 mils) of apparent wear occurred in the 2-in. pipe of the EC loop. For comparison, Table II also gives direct-wall-contact measurements; the agreement is excellent for the 1-1/2-in. piping and satisfactory for the 2-in. pipe. (In the latter case, the two sets of direct-contact measurements may not have been made at precisely the same positions.)

It may be further observed from Table II that an apparent wear peak exists in each monitored bend of the 1-1/2-in. piping and that the peaks are broad: The downstream edges of the wear peaks within the bends have not yet been observed. The shapes of these peaks will be more fully examined during the next direct-contact opportunity.

Table III shows direct-contact results from the 2-in. piping in the preheater at ambient temperature. Wear of 0-0.10 mm (0-4 mils) by mid-January 1980 was indicated, and wear values are probably correct within 0.05 mm (2 mils).

Table IV summarizes the scanner data from the experimental waveguides at the preheater. At ambient temperature, the indicated wear by mid-January was comparable to that determined from direct-contact measurements (Table III). Measured values were virtually unchanged by the de-coking treatment later in January (Table IV). For data obtained with the preheater operating at temperature, some minor changes in the method of specifying the acoustic correction temperatures, especially for waveguide no. 28, appear to be needed (Table IV).

Plant operations were resumed after the brief shutdown in January, and the progress of the erosive wear is being followed during operations by means of the scanner. Relatively low erosion rates are indicated and will be verified during the next shutdown period in early May. The erosion rates may be reduced by the presence of a thin film, probably of metal carbide, that has been noted on inner surfaces of coal liquefaction process piping by SRC pilot plant personnel. The film properties are currently being investigated.

(b) Morgantown Energy Technology Center Gasification Plant

A visit was made to the Morgantown (West Virginia) Energy Technology Center (METC) in March 1980 to test the ANL erosion scanner that is monitoring the erosive wear of an effluent cyclone separator on METC's stirred-bed coal gasifier. The scanner was operated manually during the visit to survey the array of ultrasonic monitoring sites with the cyclone at ambient temperature. The results, when compared with those of a similar survey made immediately before the most recent period of gasifier operation (November 28-December 9, 1979), reveal the wear produced during the run. These results, given in Table V, show that the wear profile for the run was similar to the cumulative profile observed earlier and described in the previous report.[3]

The ANL strip-chart recording of scanner and temperature data taken during the subject run has been analyzed. The results suggest that the rate of wear was nonuniform, and possible causes of the apparently intermittent wear are being investigated.

TABLE II. Ultrasonic Wall-thickness Measurements[a] of Erosion-Corrosion Loop Piping at SRC Pilot Plant

Position on Loop Extrados	Wall Thickness, mils (Direct-contact Data)			Change in Wall Thickness,[b] mils (Scanner Data)
	9/19/79	1/18/80	Change	
1-1/2-in. Pipe				
Upstream & contacting weld of WG 1	383	383	0	
At WG 1				-4
Midway between WGs 1 & 2	381	375	-6	
At WG 2				-6
Midway between WGs 2 & 3	380	374	-6	
At WG 3				-8
Midway between WGs 3 & 4	383	clamp	-	
At WG 4				-8
Midway between WGs 4 & 5	384	376	-8	
At WG 5				-8
Midway between WGs 5 & 6	384	376	-8	
At WG 6				-10[c]
7				-2
8				-3
9				-2
10				-6
11				-5
12				-2
2-in. Pipe				
16				-1
17				-1
18				-
19				-1
20				-2
21				-
22				-3
Upstream & near weld of WG 23	399	400	(+1)	
At WG 23				-1

TABLE II. Ultrasonic Wall-thickness Measurements[a] of Erosion-Corrosion Loop Piping at SRC Pilot Plant (continued)

Position on Loop Extrados	Wall Thickness, mils (Direct-contact Data)			Change in Wall Thickness,[b] mils (Scanner Data)
	9/??/79	1/18/80	Change	
2-in. Pipe (contd.)				
Downstream, contacting WG 23	399	398	-1	
Upstream, " " 24	399	403	(+4)	
At WG 24				-1
Downstream, " " 24	399	400	(+1)	
Upstream, " " 25	399	405	(+6)	
At WG 25				-
Downstream, " " 25	399	401	(+2)	
Upstream, " " 26	395	396	(+1)	
At WG 26				-1
Downstream, " " 26	395	393	-2	
Upstream, " " 27	393	393	0	
At WG 27				0

[a]Type 304 stainless steel calibration basis is employed. Data shown are corrected for instrument zero drift. Waveguide (WG) positions were specified in the previous report.[3] 1 mil = 0.001 in. = 0.0254 mm.

[b]10/16/79-1/17/80.

[c]Value after correction by one $\lambda/2$.

TABLE III. Wall Thickness of SRC Preheater Piping Near Waveguide Sites, as Measured Ultrasonically by Direct-wall-contact Method[a]

Position	Wall Thickness, mils		
	9/22/79	1/16/80	Change
Above WG 28	330	329	-1
Below	334	332	-2
Upstream	333	331	-2
Downstream	331	329	-2
Above WG 29	317	318	(+1)
Below	313	312	-1
Upstream	(weld)	-	-
Downstream	314	314	0
Above WG 30	325	(not read)	-
Below	320	(not read)	-
Upstream	321	321	0
Downstream	321	318	-3
Above WG 31	317	313	-4
Below	307	306	-1
Upstream	309	309	0
Downstream	309	307	-2

[a]Type 304 stainless steel calibration basis is employed. Data shown are corrected for instrument zero drift. Waveguide (WG) positions were specified in the previous report.[3] 1 mil = 0.001 in. = 0.0254 mm.

TABLE IV. Results from Experimental Waveguides[a] on SRC Preheater

Date	Waveguide No.	Temperature, °C	Distance[b], mils	Apparent Change, mils (Noncumulative)
11/1/79	28	ambient	624	Baseline
	29	"	606	"
	30		617	"
	31	"	608	"
During Operation:[c]				
12/11/79	28	278	618	-6
(3:15 PM)	29	361	600	-6
	30	417	613	-4
	31	-	(d)	-
12/11/79	28	278	616	-8
(5:00 PM)	29	361	604	-2
	30	417	615	-2
	31	-	(d)	-
During Shutdown Period:				
1/17/80	28	ambient	621	-3
	29	"	604	-2
	30	"	614	-3
	31	"	602	-6
After De-coking:				
1/29/80	28	ambient	620	-4
	29	"	606	0
	30	"	614	-3
	31	"	603	-5

[a]The 635-mm (25-in.)-long bimetallic waveguides, and their placement on the preheater, were described in the previous report.[3]

[b]Ultrasonically measured distances from waveguide shoulders to inner surface of pipe, after data correction for instrument zero drift, $\lambda/2$ offsets, temperature change of reference samples, and local pipe temperature (inferred from plant instrument data). Type 304 stainless steel calibration basis is employed. 1 mil = 0.001 in. = 0.0254 mm.

[c]Temperatures inferred from 4:30 PM plant instrument data.

[d]The transducer-waveguide coupling for waveguide 31 was poor in December. Satisfactory coupling was restored after repairs to this interface in January.

TABLE V. Change in METC Cyclone Separator Thickness[a] Caused by Operation in November-December 1979

Waveguide No.	Change		Waveguide No.	Change	
	mils	mm		mils	mm
1	0	0	11	-3	-0.076
2	(+1)	-	12	-1	-0.025
3	0	0	13	-2	-0.051
4	-3	0.076	14	-2	-0.051
5	-5	0.127	15	-1	-0.025
6	-3	0.076	16	-7	-0.178
7	-2	0.051	17	-10	-0.254
8	(+1)	-	18	-5	-0.127
9	0	0	19	-3	-0.076
10	-3	0.076	20	-2	-0.051
			21	-0	0

[a]Wall thicknesses measured in November 1979, compared with wall thicknesses measured in March 1980; thicknesses determined ultrasonically at waveguide sites described in Ref. 3, with cyclone at ambient temperature.

2. Refractory Installation Practices

a. Detection of Thermally Induced Acoustic Emissions from Refractory Concrete Materials

Additional progress has been made this quarter on preparation of the state-of-the-art report.

3. Component Inspection

a. Acoustic Monitoring of Valves

A field trip was made to Baytown, Texas on January 13, 1980 to visit Exxon's 250 T/day coal liquefaction plant. One purpose of this visit was to more fully develop the respective responsibilities for field testing of the ANL-developed passive acoustic system during valve leakage tests. Valves to be monitored were tentatively selected and data-acquisition equipment and field-implementable techniques discussed. Present plans call for passive acoustic data to be taken on five valves.

Tape recorders for use at the field-test site were ordered after an extensive evaluation of available instruments.

Experimental work was initiated on the use of phase correlation to eliminate background noise. Results of this work will be presented in subsequent reports. Field tests are planned to be initiated in August or September 1980.

Task D -- Corrosion Behavior of Materials in Coal-conversion Processes
(K. Natesan)

The objectives of this program are to (1) develop uniaxial tensile data on four selected commercial alloys exposed to multicomponent gas environments, (2) experimentally evaluate the high-temperature corrosion behavior of iron- and nickel-base alloys in gas environments with a wide range of oxygen, sulfur, and carbon potentials, (3) evaluate deposit-induced hot-corrosion behavior of heat-exchanger and gas-turbine materials with and without coatings after exposure to multicomponent gas environments, and (4) develop an approach, based upon available thermodynamic and kinetic information, to the evaluation of possible corrosion problems in various coal-conversion systems.

1. Uniaxial Tensile Properties

The experimental program to generate uniaxial tensile data on four iron- and nickel-base alloys exposed to multicomponent gas environments was discussed previously.[4] The experimental apparatus and the chemical composition of the alloys and gas mixtures used in this program were described in detail.[5] Calculated values for the oxygen and sulfur partial pressures established by the gas mixtures in different runs have also been reported.[6]

During the current reporting period, corrosion and uniaxial tensile specimens are being examined by scanning-electron microscopy and an electron microprobe to evaluate the depths of scale and intergranular penetration in various specimens. An analysis of the tensile test results indicated a decrease in tensile properties such as yield and ultimate tensile strength as the oxygen partial pressure in the preexposure environment was lowered. The results also showed that the data generated on specimens exposed at 1 atm total pressure in Argonne National Laboratory experiments were similar to those generated at 34 and 102 atm in the Battelle-Columbus Laboratories program.[7] Consequently, it can be concluded that the effect of system pressure on the tensile properties is negligible if the influence of total pressure on the gas chemistry is correctly accounted for in the analysis. The results obtained in this program will be summarized in a topical report.

2. Corrosion Rates of Commercial Alloys

The long-term corrosion behavior of a number of Fe-, Ni-, and Co-base alloys in a mixed-gas environment is being evaluated in the Metals Properties Council (MPC) program at IIT Research Institute (IITRI).[8] Figure 9 shows the compositions of the various Fe- and Ni-base alloys that have been exposed to multicomponent gas mixtures at temperatures up to 982°C. The majority of experiments in this program are conducted at a fixed oxygen partial pressure while the sulfur in the gas is varied from 0 to 1.0 vol. % H_2S (see Table VI for the O, S, and C potentials). In general, weight loss/gain data were obtained for the specimens after exposure to complex gas mixtures; subsequently, the specimens were metallographically examined to evaluate the scale thicknesses and alloy penetration depths in the materials. A summary of experimental conditions used in the IITRI corrosion test program is given in Table VII. Exposures of 10,000 h duration, at 982°C in the MPC-selected gas mixture containing 0.5 vol. % H_2S and at 899°C with 1.0 vol. % H_2S, have been completed. The experiments at 982°C with 1.0 vol. % H_2S and at 899°C with 0.5 vol. % H_2S are in progress. Exposures of 1000 h duration have been completed at 816°C in gas mixtures containing 0.1, 0.5, and 1.0 vol. % H_2S. In order to evaluate the effect of a lower pO_2 than that established by the MPC-selected gas mixture, 1000-h exposures have been conducted at 982°C with 0.5 vol. % H_2S and 20 vol. % H_2O (instead of 39.5 vol. % H_2O). Table VII also lists the values of the excess oxygen partial pressure ratios ($p_{O_2}/p_{O_2}{}^e$) established in different experiments. It can be concluded from the information presented in earlier reports[9,10] that excess pO_2 ratios in the range used in these experiments (10^3 to 10^5) will result in oxide-mode interaction for the Fe-, Ni-, and Co-base alloys with high concentrations of chromium; the effect of long exposure times (up to 10,000 h) will establish the susceptibility of a given alloy to breakaway corrosion.

The effect of variation in H_2S concentration in the range 0 to 1.0 vol. % on the corrosion behavior of a number of commercial materials has been evaluated after 1000-h exposure at 982°C. The results, plotted in Fig. 10 as metal loss vs excess oxygen parameter, show an increase in corrosion as the H_2S concentration in the gas phase increases. Figure 11 shows the scale thickness and alloy penetration depth as a function of the excess oxygen parameter for a number of alloys that exhibit significant corrosion in H_2S-containing atmospheres. The thicknesses of scales developed on these

alloys (except RA330 and HD45) are large even with 0.1 vol. % H_2S in the gas phase, conditions under which the high-chromium alloys should develop protective oxide layers. It is evident that these alloys show poor oxidation resistance (see data points for 21-6-9, HC-250, 309, etc.), which is improved by an increase in the H_2S content of the gas phase. However, these alloys will be unsuitable for application in coal-conversion systems because they develop thick scales under low-H_2S conditions (typical of low-S coal feedstock) and exhibit substantial intergranular sulfur penetration under high-H_2S conditions (typical of high-S coal feedstock).

Because complex alloys exposed to multicomponent gas environments may develop a protective oxide scale and at the same time exhibit significant intergranular penetration of sulfur into the substrate material, judicious selection of an alloy for use in coal-gasification systems requires data on the extent of sound-metal loss as well as weight change. Such data have been obtained for a number of primary, secondary, and alternate alloys after exposure to mixed-gas environments at temperatures of 899 and 982°C.[8] The results show that several commercially available alloys exhibit acceptable corrosion rates of $\sim$ 0.6 mm y^{-1} (24 mils y^{-1}), based on 10,000-h exposures; however, it should be noted that these corrosion experiments were conducted at excess oxygen parameter values of $\sim 10^3$ or higher (see Table VII).

The effect of variation in oxygen and sulfur partial pressures on the corrosion behavior of alloys can be evaluated by a comparison of 1000-h data on scale thickness and intergranular penetration obtained by different researchers. Natesan[4-6,10-11] obtained data on Incoloy 800 and Type 310 stainless steel with varying p_{O_2} and p_{S_2} at 982° and ambient pressure. Wright[7] obtained similar data at total pressures of 34 and 102 atm. Hill et al.[8] obtained data on these alloys for the MPC gas mixture, MPC gas modified with 20 vol. % H_2O, and low-Btu gas that included nitrogen. The data on scale thickness and alloy penetration depth from all these investigations are plotted as a function of excess oxygen parameter ($p_{O_2}/p_{O_2}^e$) in Figs. 12 and 13 for Type 310 stainless steel and Incoloy 800, respectively. In general, the results show that below an oxygen pressure threshold represented by $p_{O_2}/p_{O_2}^e \sim 10^3$, the total corrosion (scale thickness + penetration depth) of the alloys is significant. However, the data of Wright, Hill et al. (low-Btu gas), and Natesan (30 vol. % CH_4 in inlet gas) show significantly lower values of scale thickness and penetration depth for Incoloy 800 and probably for Type 310 stainless steel. In these experiments, the oxygen pressure is low enough that a protective oxide layer does not develop on the alloy; on the other hand, the carbon activity in the gas is high enough to form stable Cr-rich carbides in the alloy. As a result, the corrosion behavior of the material depends on the relative rates of formation of carbides vs sulfides in the scale. Wright has observed a hard layer of carbide on the specimens tested in these environments. Once the carbide scale layer is formed, the extent of corrosion will be determined by either the transport of sulfur through the carbide layer or by the sulfidation of carbide particles in the scale layer. Significant carburization depths have been reported by Hill et al. for specimens exposed to low-Btu gas environments. Very little fundamental information is presently available on the relative role of carbon and sulfur in the mixed-gas environment on the corrosion behavior of materials (in the absence of protective oxide scales). Since high carbon activities are expected at elevated system

pressures and at low temperatures, it is worthwhile to establish whether protective carbide layers rather than fast-growing sulfide scale can be developed on alloy surfaces.

3. Experimental Program

Deposit-induced hot-corrosion behavior of heat-exchanger and gas-turbine materials exposed to multicomponent gas environments is of considerable interest in advanced energy systems that utilize fossil fuels. For this purpose, the ongoing program includes characterization of environments in low-Btu gasification and direct-combustion processes and the evaluation of materials in complex gas mixtures that simulate normal operating conditions and off-normal excursion situations in these processes.

To simulate the air and stream tubes exposed in an environment arising from combustion of coal or coal-derived fuels, tube specimens that are internally cooled with air or inert gas are used in a series of corrosion experiments. Figure 14 shows the experimental setup, in which four individually operated systems are used for the exposure of tube specimens. Figure 15 shows a close-up view of one of the four systems, and Fig. 16 shows the details of the corrosion probe. The probe is approximately 40 cm in length, with a specially designed head that incorporates the cooling-fluid path and thermocouples. The temperature in the mixed-gas environment is measured by a Chromel-Alumel couple inserted in the thermowell. In the first few experiments, thermocouples are also spot-welded onto the outer and inner surfaces of tube specimens. Another couple is inserted in the cooling fluid inside the specimen assembly. During a run, the outputs from these couples are continuously recorded on a strip chart. Figure 17 shows the details of tube specimens in the unassembled and assembled configurations with the thermocouples in the attached position. At present, experiments are being conducted at a metal temperature of 593°C in mixed-gas environments with low oxygen partial pressures and as a function of sulfur partial pressure.

TABLE VI. Reaction Potentials Established at IITRI in Experimental Runs Conducted at Different Temperatures

Temperature, °C	System Pressure, atm	Gas Composition, vol. %							Reaction Potentials		
		CO	CO_2	CH_4	H_2	H_2O	H_2S	NH_3	p_{O_2}, atm	p_{S_2}, atm	a_c
982	68	18	12	5	24	40	0	1.0	1.3×10^{-15}	-	0.195
		18	12	5	24	39.9	0.1	1.0		3.1×10^{-8}	
		18	12	5	24	39.5	0.5	1.0		7.6×10^{-7}	
		18	12	5	24	39	1.0	1.0		3.1×10^{-6}	
		18	12	5	24	38.5	1.5	1.0		6.8×10^{-6}	
899	68	18	12	5	24	40	0	1.0	6.4×10^{-17}	-	0.360
		18	12	5	24	39.9	0.1	1.0		1.3×10^{-8}	
		18	12	5	24	39.5	0.5	1.0		3.2×10^{-7}	
		18	12	5	24	39	1.0	1.0		1.3×10^{-6}	
		18	12	5	24	38.5	1.5	1.0		2.9×10^{-6}	
816	68	18	12	5	24	40	0	1.0	2.6×10^{-18}	-	0.387
		18	12	5	24	39.9	0.1	1.0		5.4×10^{-9}	
		18	12	5	24	39.5	0.5	1.0		1.4×10^{-8}	
		18	12	5	24	39	1.0	1.0		5.5×10^{-7}	
		18	12	5	24	38.5	1.5	1.0		6.2×10^{-6}	
650	68	18	12	5	24	40	0	1.0	8.2×10^{-22}	-	0.782
		18	12	5	24	39.9	0.1	1.0		8.8×10^{-10}	
		18	12	5	24	39.5	0.5	1.0		2.2×10^{-8}	
		18	12	5	24	39	1.0	1.0		8.8×10^{-8}	
		18	12	5	24	38.5	1.5	1.0		2.0×10^{-7}	

TABLE VII. Summary of Experimental Conditions Used in IITRI Corrosion Test Program

Temp., °C	Total Pressure, atm	Vol. % H_2S in Gas Mixture[a]	Exposure Time, h	p_{O_2}, atm	p_{S_2}, atm	a_c	$p_{O_2}/p_{O_2}^e$
982	68	0.5	10000	1.3×10^{-15}	7.6×10^{-7}	0.195	3.6×10^{3}
		1.0	10000[b]	1.3×10^{-15}	3.1×10^{-6}	0.195	9.6×10^{2}
899	68	1.0	10000	6.4×10^{-17}	1.3×10^{-6}	0.360	2.0×10^{3}
		0.5	10000[b]	6.4×10^{-17}	3.2×10^{-7}	0.360	7.2×10^{3}
816	68	0.1	1000	2.6×10^{-18}	5.4×10^{-9}	0.387	2.1×10^{5}
		0.5	1000	2.6×10^{-18}	1.4×10^{-8}	0.387	1.1×10^{4}
		1.0	1000	2.6×10^{-18}	5.5×10^{-7}	0.387	3.3×10^{3}
982	68	0.5[c]	1000	5.8×10^{-16}	8.1×10^{-7}	0.465	1.5×10^{3}

[a] MPC-selected gas composition.

[b] These experiments have accumulated ~ 3000 h.

[c] H_2O content in the gas was 20 vol %, rather than 39.5 vol. % as in the MPC-selected mixture.

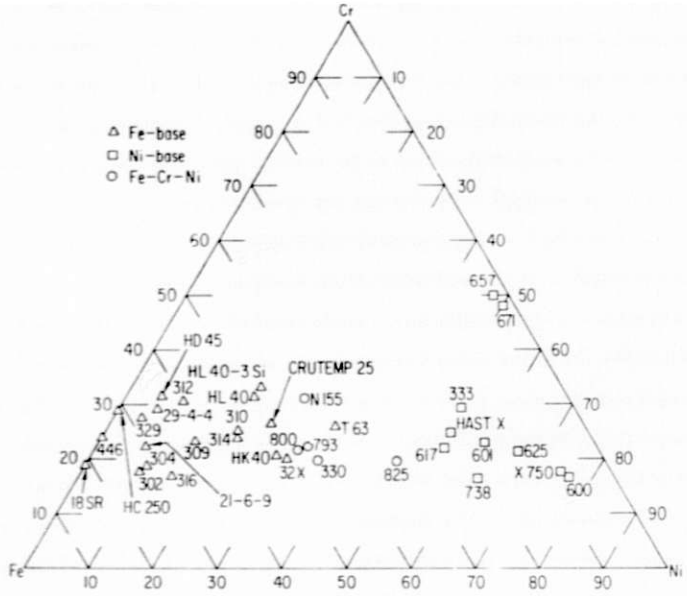

Fig. 9. Ternary Fe-Cr-Ni Diagram Depicting Various Fe- and Ni-base Alloys that have been Corrosion Tested in Complex Gas Environments. ANL Neg. No. 306-79-30.

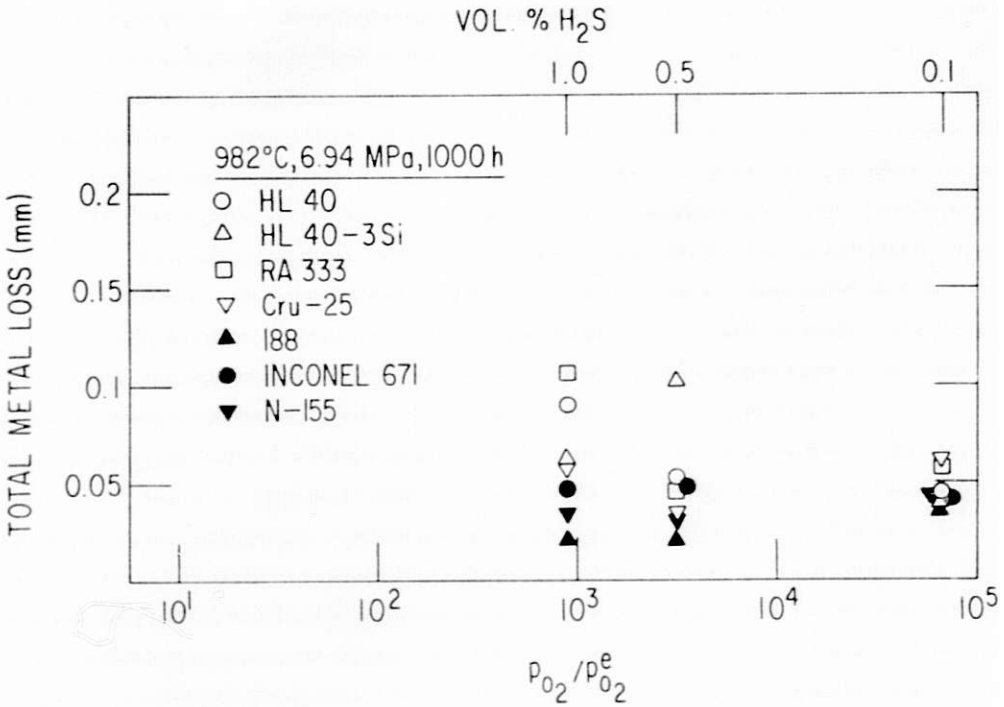

Fig. 10. Total Metal Loss as a Function of Excess Oxygen Parameter for Alloys Exposed for 100 h to MPC-selected Gas Mixture with 0.1 to 1.0 vol. % H_2S at 982°C and 6.94 MPa. ANL Neg. No. 306-79-1052.

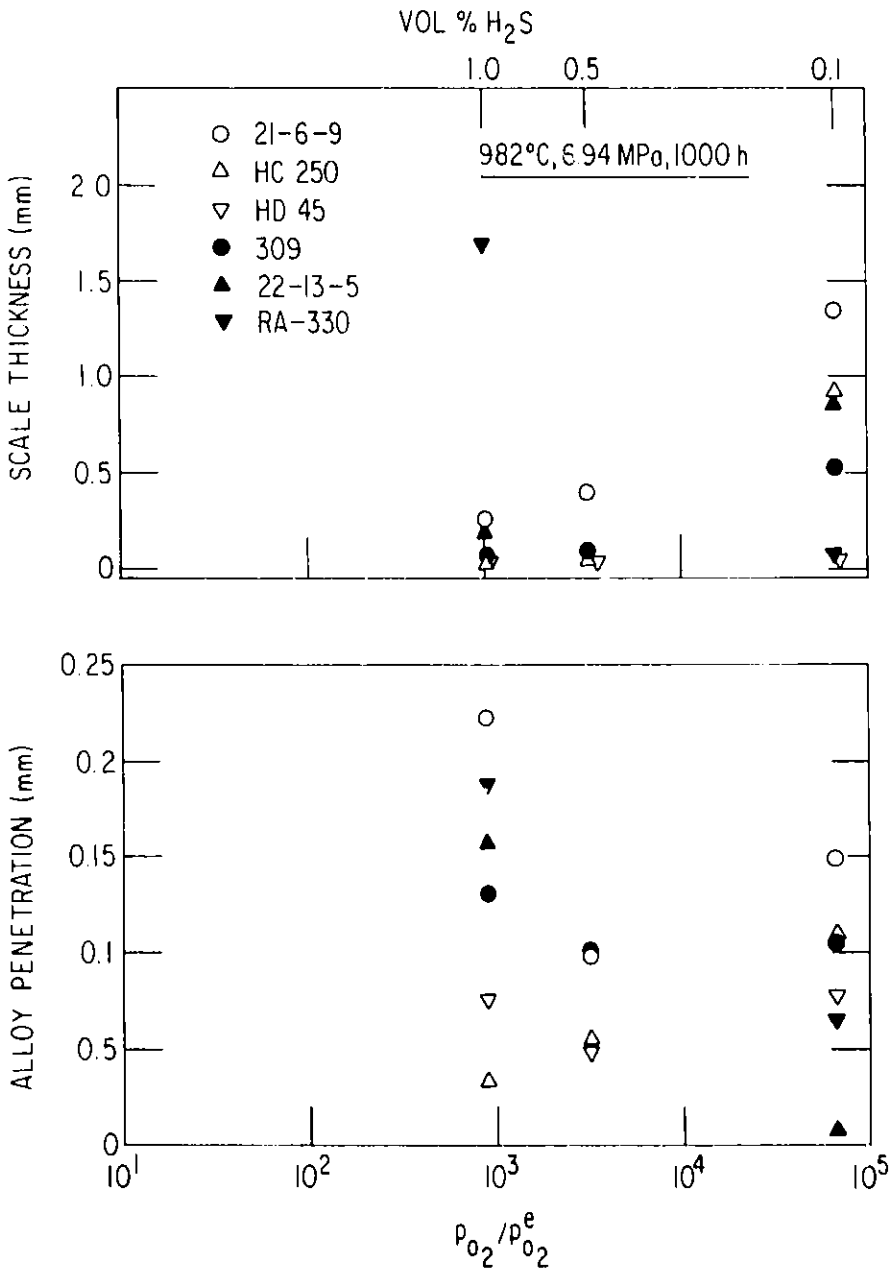

Fig. 11. Scale Thickness and Alloy Penetration Depth as a Function of Excess Oxygen Parameter for Alloys Exposed for 1000 h to MPC-selected Gas Mixture with 0.1 to 1.0 vol. % H_2S at 982°C and 6.94 MPa. ANL Neg. No. 306-79-1058.

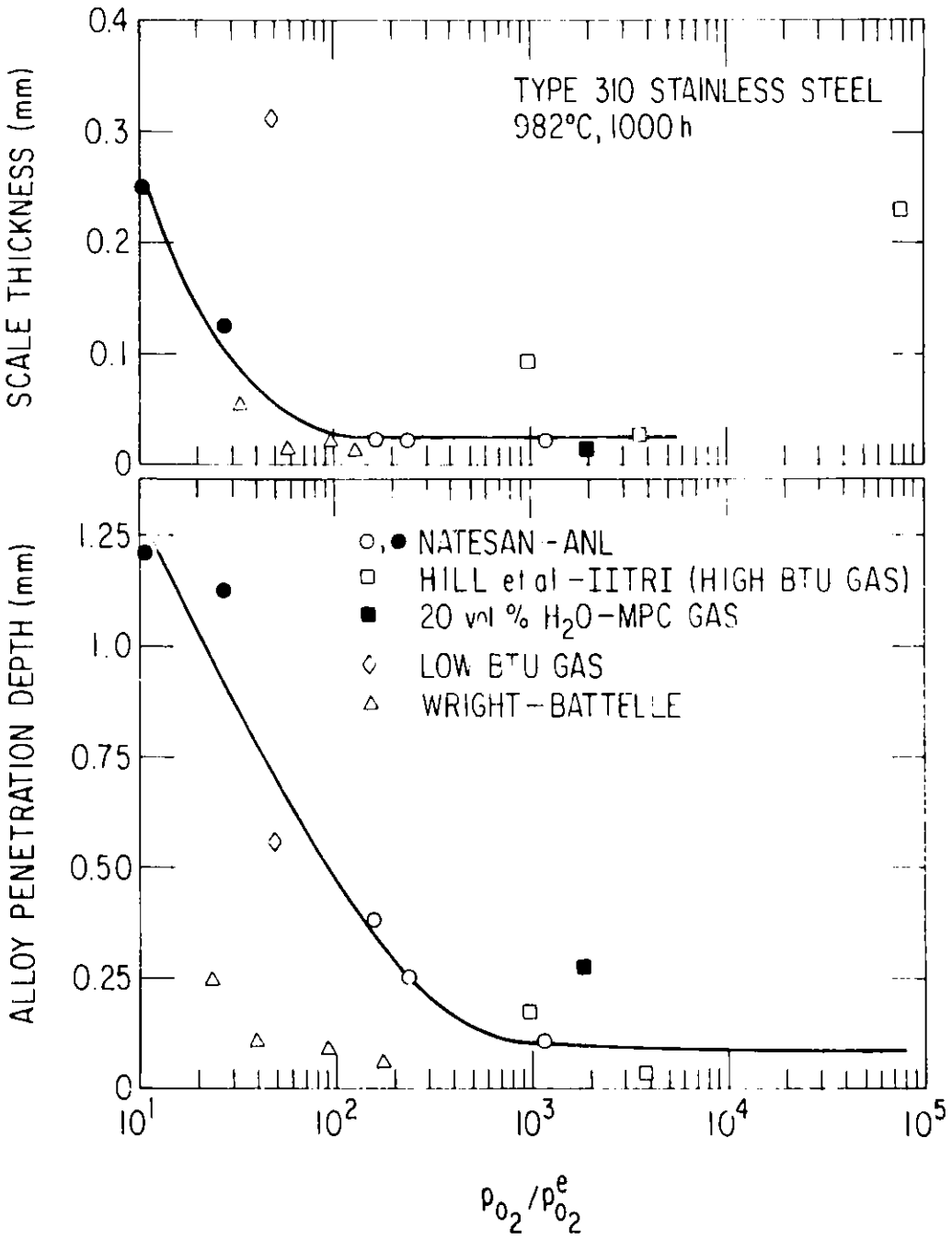

Fig. 12. A Comparison of Data on Scale Thickness and Alloy Penetration Depths for Type 310 Stainless Steel Exposed for 1000 h to Multicomponent Gas Environments at 982°C. ANL Neg. No. 306-79-1063.

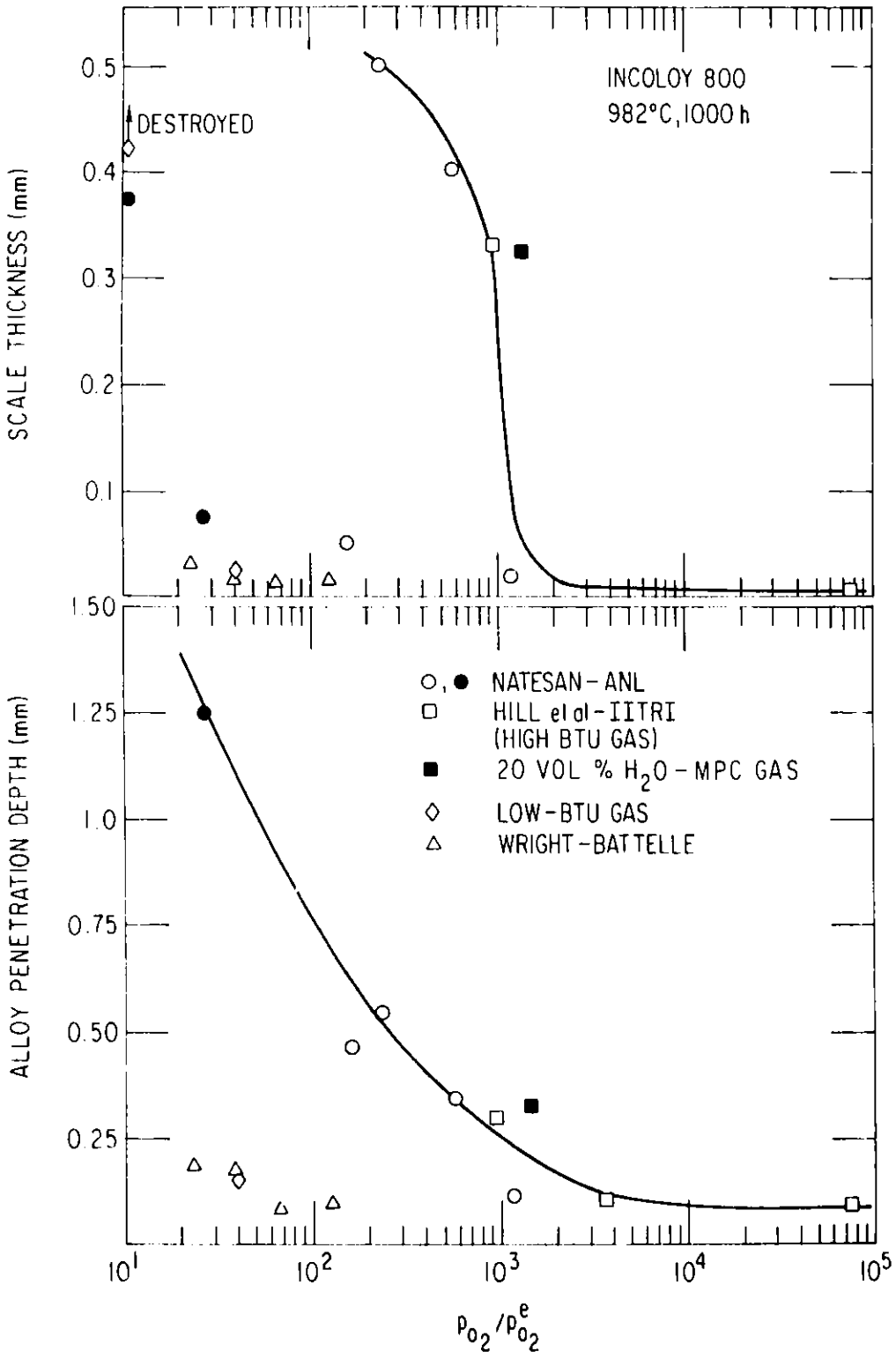

Fig. 13. A Comparison of Data on Scale Thicknesses and Alloy Penetration Depths for Incoloy 800 Exposed for 1000 h to Multicomponent Gas Environments at 982°C. ANL Neg. No. 306-79-1070.

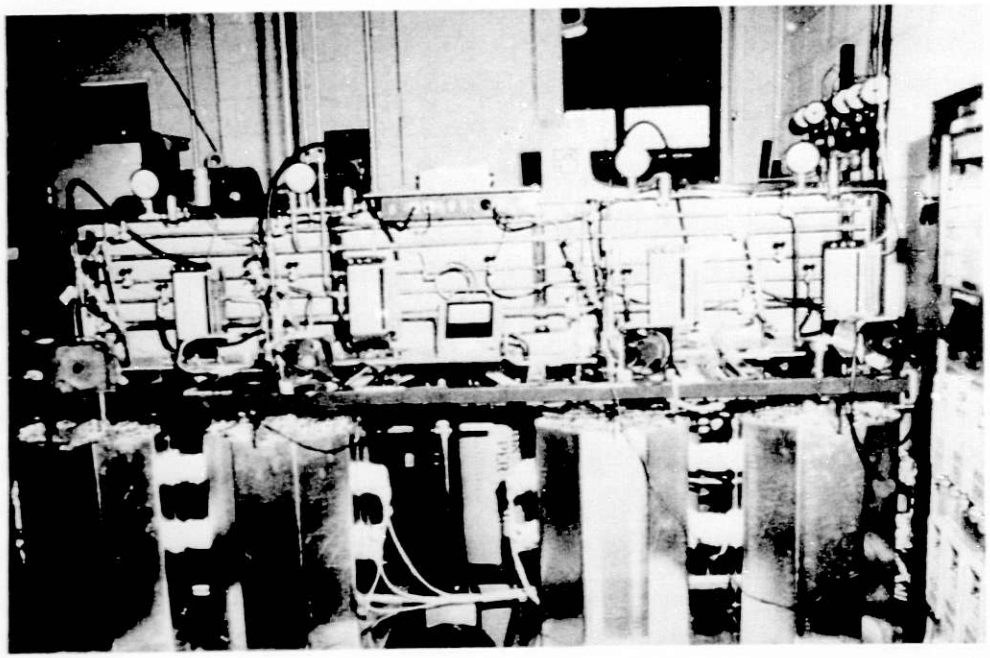

Fig. 14. Experimental Setup with Four Individually Operable Systems for the Exposure of Tube Specimens. ANL Neg. No. 306-80-204.

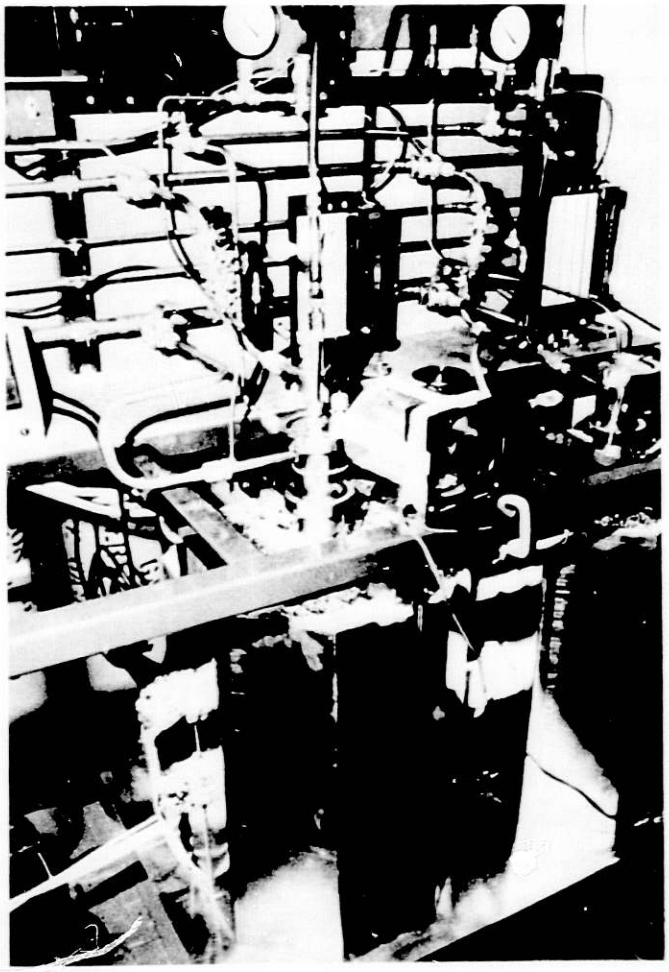

Fig. 15. A Closeup View of One of the Systems Used in Corrosion Studies. ANL Neg. No. 306-80-206.

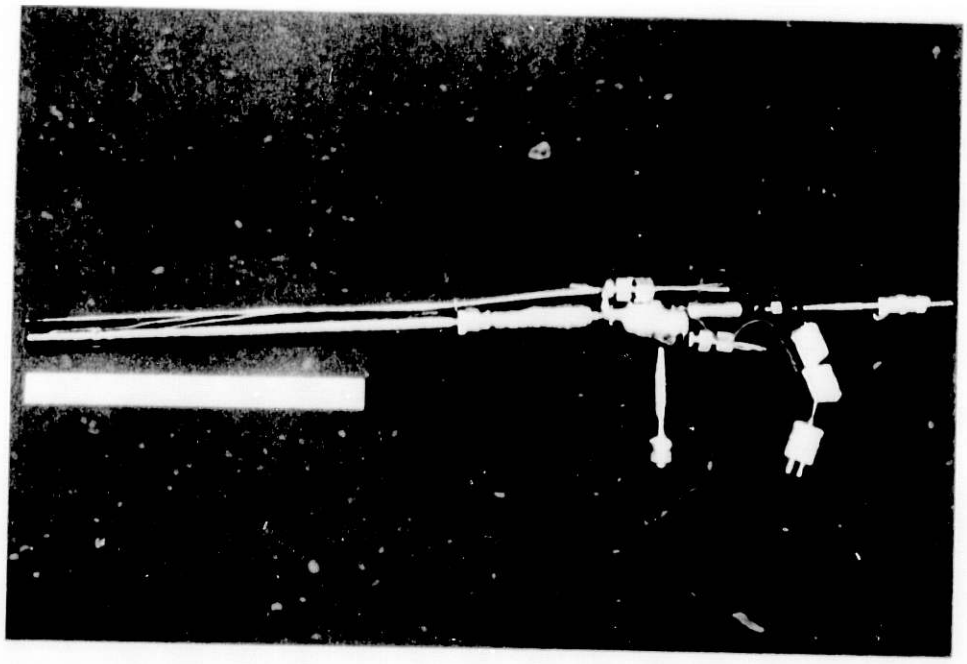

Fig. 16. Photograph Showing the Details of a Corrosion Probe. ANL Neg. No. 306-80-205.

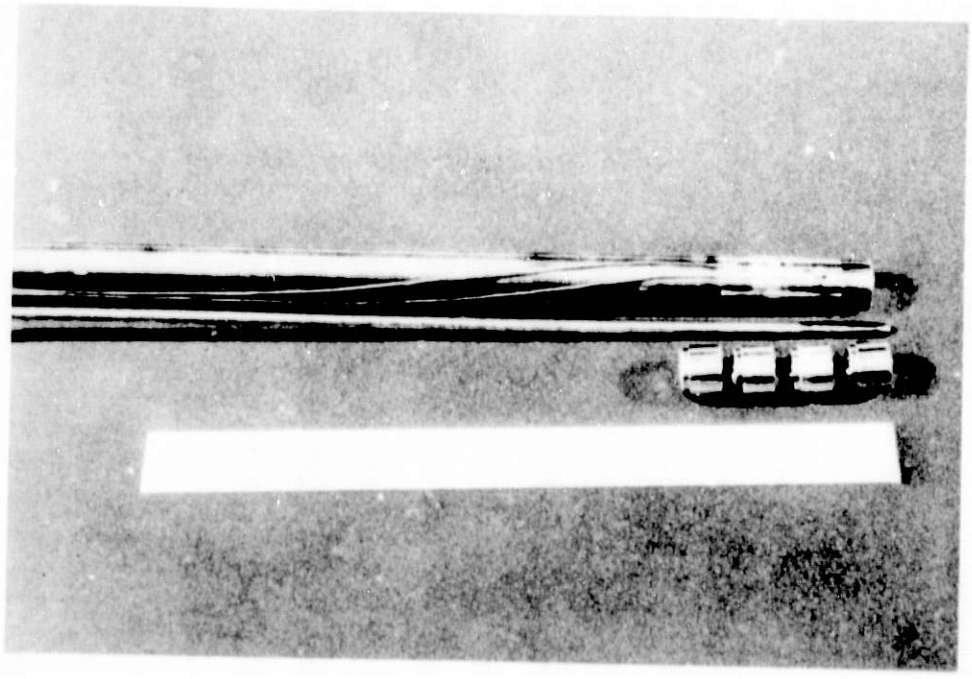

Fig. 17. Details of Tube Specimens in the Unassembled and Assembled Configurations with Thermocouples in the Attached Position. ANL Neg. No. 306-80-212.

Task E -- Erosion Behavior of Materials in Coal-conversion Processes
(J.Y. Park and W.J. Shack)

The objectives of the erosion program at ANL are to develop an engineering data base and the necessary analytical tools for rational design of components subject to erosive wear in coal-conversion plants. Engineering design data will be obtained from erosion tests which will be performed at temperatures and in atmospheres designed to simulate actual plant conditions. The laboratory results will be compared with in-situ measurements currently being obtained from the NDT program at ANL.

Corrosion and erosion calibration tests on 1015 carbon steel (CS), Type 304 stainless steel (SS), Incoloy 800, and Stellite 6B were performed. Corrosion calibration tests in a simulated gasifier atmosphere (CO 18, CO_2 12, CH_4 5, H_2 24, H_2O 39, NH_3 1, H_2S 1 in vol. %) at 816°C were reported previously.[1,3] These tests were repeated to ensure reproducibility of the results. Significant amounts of corrosion were observed in all alloys. Cross sections of the specimens were examined by optical metallography, and material degradation due to corrosion was measured in terms of weight change, loss of substrate thickness, scale formation, and internal corrosion. The results of these corrosion calibration tests are similar to those presented in previous reports.[1,3]

A new specimen holder was built to provide more accurate control of particle impingement angle. Up to forty specimens can be mounted for a single test. A room-temperature erosion calibration test was performed on 1015 CS, Type 304 SS, Incoloy 800, RA310 SS and Stellite 6B specimens using the new specimen holder and 100-grit size (150-μm) alumina at an impingement velocity of 22 m/s and angles 6-36°. Erosion rate (mass loss/mass impacted) was calculated from weight loss, and the results are shown in Table VIII. The rate is in the range of 0.03-0.09 mg/g, which is about 7 times lower than that obtained in earlier tests at 70 m/s using 240-grit size (50-μm) alumina.[6] However, the variation is consistent with the expected dependence of erosion rate on velocity.

During the next quarter, a few additional erosion calibration tests will be completed at higher impingement angles, and erosion-corrosion calibration tests will be performed in the simulated gasifier atmosphere at 816°C. An external feed reservoir with a level indicator will be installed in order to perform continuous long-term erosion-corrosion tests. (The current internal feed reservoir capacity, 25 kg of alumina, limits tests to ∿ 50 h unless very low particle fluxes are used.)

TABLE VIII. Erosion Calibration Test[a] Results

Material	Impingement Angle			
	6°	16°	24°	36°
1015 Carbon Steel	0.09[b]	0.05	0.06	0.03
Type 304 Stainless Steel	0.06	0.03	0.04	0.03
Incoloy 800	0.06	0.05	0.05	0.04
RA310 Stainless Steel	0.03	0.04	0.04	0.03
Stellite 6B	0.06	0.04	0.04	0.03

[a]Air atmosphere at room temperature.
[b]Erosion rates in mg/g.

Task F -- Failure Analysis *(D.R. Pierocks, S. Greenberg, J.Y.N. Wang, G.M. Dragel and J.E. Slattery)*

1. Experimental Thermowells for IGT Ash Agglomerating Gasifier

Seven experimental thermowells have been prepared for trial exposure in the IGT Ash Agglomerating Gasifier (U-Gas) Pilot Plant. The bottom portions of these thermowells, which will see the most severe conditions in service, were fabricated using several combinations of alloys and coatings as summarized in Table IX. The Cr-Si and Cr-Al-Hf coatings were applied by the Lockheed Research Laboratories of Palo Alto, CA using a slurry fusion process, and the aluminized coatings were applied by Alon Processing, Inc. of Tarentum, PA. In all cases, the upper portions of the thermowells were fabricated of uncoated Type 304 stainless steel with carbon steel mounting flanges.

After leak testing and radiographic inspection of the welds, the completed thermowells were delivered to personnel at the U-Gas Pilot Plant in February. The principal objective in testing the trial alloys and coatings is to determine their resistance to high-temperature sulfidation, with less emphasis on their resistance to erosion by particles in the gasifier fluidized bed. Accordingly, the test plan calls for exposing the thermowells at locations somewhat above the operating height of the bed, but still in the high-temperature portion of the gasifier. Only three locations satisfying these requirements are available, and thermowells 2 through 7 will be exposed in these locations in two series of runs. Thermowell 1, which is identical with thermowell 2, will be tested at a different location in the gasifier near the top of the fluidized bed under conditions of combined erosive wear and sulfidation.

At present, experimental thermowells 2, 3, and 7 have been installed at positions approximately 1.1, 1.4, and 2.3 m (3.5, 4.5, and 7.5 ft) above the normal operating height of the bed, and thermowell 1 has been installed approximately 0.4 m (1.4 ft) above the top of the bed. However, the plant has not been operated subsequent to the installation of the thermowells, and the schedule for the resumption of operations is uncertain at this time.

2. Tubing and Compressor Diaphragm Assembly Samples from Grand Forks Energy Technology Center

An examination of tubing bend and compressor diaphragm samples from the Grand Forks Energy Technology Center coal-liquefaction continuous-process unit has been completed. The tubing samples consist of two Type 316 stainless steel bends (14.3 mm OD) from a line connecting the autoclave reactor to the high-temperature slurry-gas separator. The compressor diaphragm set consists of an inner and outer ply made of Type 316 stainless steel and a center ply made of Type 301 stainless steel. A more complete description of these components and their operating environments is provided in a previous report.[3]

The results of this examination may be summarized as follows:

1. A thorough examination of the ID of the tubing bends indicates that no cracking is esent.

2. Through-wall cracks have been cted in both the diaphragm in contact with the ga and the diaphragm in contact with hydraulic fluid. No cracking was observed in the center diaphragm.

3. The cracking in the compressor diaphragm in contact with the gas apparently initiated on the gas side. In the case of the diaphragm in contact with the hydraulic fluid, cracking initiated on the fluid side in an area of localized pitting.

3. Solids Transfer Line from IGT HYGAS Pilot Plant

Portions of a corroded and perforated solids transfer line from the IGT HYGAS coal gasification pilot plant have been sent to Argonne for analysis. The failed line runs vertically approximately down the center of the gasifier reactor vessel, and is used to transport char particles at low velocities (< 1 m/s) from the second (high-temperature reactor) stage of the vessel to the third (steam-oxygen gasifier) stage. The line is made of 7.6-cm (3-in.)-ID Schedule 80 pipe welded together at several points along its length using 7.6-cm (3-in.)-long, 9.5-cm (3.75-in.)-ID Schedule 120 sleeve couplings. The ends of the couplings are slipped over the ends of the pipe sections to be joined and circumferentially welded to them. The piping material and weld couplings are specified to be RA 330, and the weld filler metal used to join the pipe to the couplings is Inconel 182. The total length of the transfer line is about 8.2 m (26.8 ft), and it is terminated by a hot-char valve at the outlet end in the steam-oxygen gasifier zone. The line is supported inside the reactor vessel by means of a flat plate welded to the pipe about two-thirds of the way up its length. This flat plate rests on a refractory grid support structure between the second and third stages of the vessel. A pair of bolted flanges are used to provide a mechanical joint in the line immediately above the grid support plate.

The operating conditions of the HYGAS pilot plant over the last several years since the present line was installed have been somewhat variable, largely because of the variety of feedstocks employed. However, a representative average gas composition from the steam-oxygen gasifier stage, after equilibration at room temperature, is given by the analysis (in mole percent) 56.9 H_2O, 16.9 H_2, 16.2 CO_2, 8.0 CO, 1.9 CH_4, and 0.1 H_2S. The operating temperature along the length of the transfer line varies from about 870-980°C (1600 to 1800°F) in the steam-oxygen gasifier zone to about 540-820°C (1000 to 1500°F) in the high-temperature reactor zone.

A visual examination of the failed components revealed that, in all cases, failure had occurred at welds. Three of the failures were located at weld couplings, one at a welded junction with a smaller-diameter line, and one each at the welds connecting the support plate and coupling flange to the line. In all cases, failure was due to corrosive attack of the weld metal

and adjacent base metal from the OD. Complete perforation occurred at a minimum of three locations.

Figure 18 shows the macroscopic appearance of a failed welded coupling after initial axial sectioning. Attack on the weld filler metal and adjacent base metal at both ends of the coupling is apparent, with complete penetration of the pipe wall visible on the right-hand side of the figure. The general features observed in the macroscopic examination of the remaining failure locations were rather similar. Failure invariably occurred by attack of the weld filler metal from the OD, generally followed by spread of the corrosive attack into the adjacent base metal. Less severe weld-metal attack was noted in the portion of the line located in the high-temperature reactor zone, where the operating temperatures tended to be somewhat lower. No significant base-metal attack was observed in any of the samples examined except as an immediate consequence of adjacent weld-metal attack.

Metallographic examination of sections taken from the failed components typically reveals considerable surface and internal oxidation and sulfidation below the outer corrosion-product layer. Figure 19 shows the intergranular and twin-boundary attack observed in the base metal adjacent to an attacked weld-metal region. X-ray analysis identifies both chromium oxide and sulfide phases in the grain and twin boundaries, with the probable precipitation of the $M_{23}C_6$ carbide inside the grains. The corrosion-product scale is found to consist of chromium and iron oxides as well as significant amounts of nickel sulfide.

The present failure is tentatively attributed to severe sulfidation of the high-nickel (~ 67 wt. %) Inconel 182 weld filler metal in the HYGAS operating environment. Both the x-ray analyses and the morphology of the surface scale indicate that the low melting point $Ni\text{-}Ni_3S_2$ eutectic was formed as one of the corrosion products at the surface of the weld metal. Since the operating temperature of the transfer line was generally well in excess of the 635°C (1175°F) melting point of this eutectic, the surface corrosion product was at least partly liquid during operation. This liquid phase would tend to inhibit the formation of a protective Cr_2O_3 layer on the contacting metal surface as well as to flux away any oxide already present. The weld metal and adjacent base metal would thus be susceptible to further sulfidation as well as internal oxidation, as seen in Fig. 19. Alternative lower-nickel weld filler metals appropriate for the present application are currently being explored.

4. Thermocouple from IGT HYGAS Pilot Plant

A failure analysis has been initiated on samples from a thermocouple taken from the IGT HYGAS coal gasification pilot plant. The failed thermocouple is a Type K (chromel/alumel) device with a Type 310 stainless steel sheath and MgO insulation. The sheath ruptured after approximately 361 hours of service in the steam-oxygen gasifier zone of the HYGAS reactor at temperatures ranging from 871 to 982°C (1600 to 1800°F) and pressures of from 3.5 to 4.5 Mpa (500 to 650 psi). The thermocouple was not protected by a thermowell. Initial x-ray diffraction results indicate that the conversion of the MgO insulation to $Mg(OH)_2$ in the failed regions, and the

accompanying volume expansion, undoubtedly contributed to further splitting of the sheath. However, the causes of the initial sheath penetration and rupture are still under investigation.

TABLE IX. Summary of Alloys and Coatings Used to Fabricate Lower Portions of Experimental Thermowells

Thermowell No.	Alloy	Coating
1	Haynes 188	none
2	Haynes 188	none
3	Incoloy 800	Cr-Al-Hf
4	Incoloy 800	aluminized
5	Type 310 stainless steel	Cr-Si
6	Type 310 stainless steel	Cr-Al-Hf
7	Type 310 stainless steel	aluminized

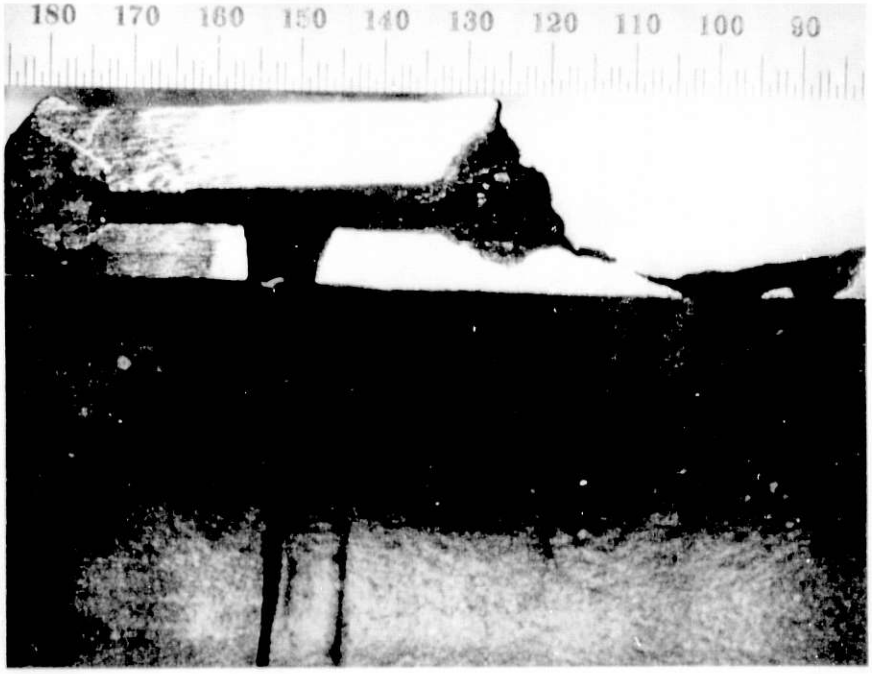

Fig. 18. Macroscopic Appearance of Failed Weld Coupling from HYGAS Internal Solids Transfer Line. ANL Neg. No. 306-80-208.

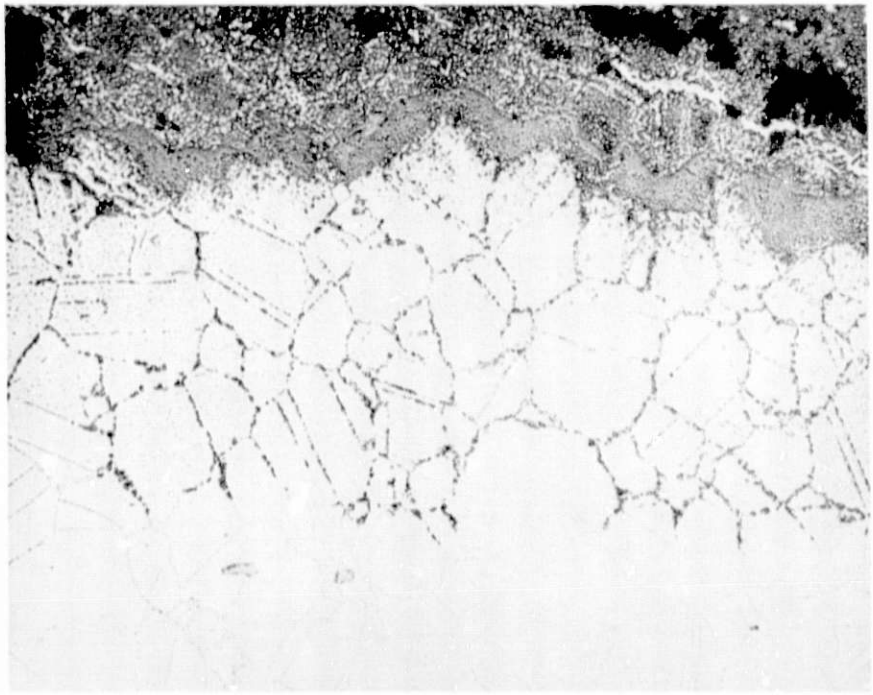

Fig. 19. Corrosive Attack of Base Metal Adjacent to Weld in Coupling from HYGAS Internal Solids Transfer Line. ANL Neg. No. 306-80-207.

REFERENCES

1. Materials Technology for Coal-conversion Processes, Eighteenth Quarterly Report, April-June 1979, Argonne National Laboratory, ANL-79-93, pp. 1-10.

2. E.M. Levin and H.F. McMurdie, Phase Diagrams for Ceramists, 1975 Supplement, The American Ceramic Society, Columbus, OH (1975) p. 280.

3. Materials Technology for Coal-conversion Processes, Nineteenth Report, July-December 1979, Argonne National Laboratory, ANL-80-12.

4. Materials Science Division Coal Technology Ninth Quarterly Report, October-December 1976, Argonne National Laboratory, ANL-77-5.

5. Materials Technology for Coal-conversion Processes, Thirteenth Quarterly Report, January-March 1978, Argonne National Laboratory, ANL-78-54.

6. Materials Technology for Coal-conversion Processes, Fourteenth Quarterly Report, April-June 1978, Argonne National Laboratory, ANL-78-79.

7. I.G. Wright, "Correlation of the High Temperature Corrosion Behavior of Structural Alloys with the Components of Coal Conversion Environments," Battelle-Columbus Laboratories, private communication.

8. V.L. Hill and B.A. Humphreys, "A Program to Discover Materials Suitable for Service Under Hostile Conditions Obtained in Equipment for the Gasification of Coal and Other Solid Fuels," Metals Properties Council Reports, FE-1784-45, -48, -51, -54, A.O. Schaefer, Ed., 1978 and 1979.

9. Materials Technology for Coal-conversion Processes, Twelfth Report, July-December 1977, Argonne National Laboratory, ANL-78-6.

10. Materials Technology for Coal-conversion Processes, Sixteenth Quarterly Report, October-December 1978, Argonne National Laboratory, ANL-79-23.

11. Materials Technology for Coal-conversion Processes, Fifteenth Quarterly Report, July-September 1978, Argonne National Laboratory, ANL-79-2.